13th World Conference on Earthquake Engineering
Vancouver, B.C., Canada
August 1-6, 2004
Paper No. 736

HIGHER MODE EFFECT ON LATERAL FORCE DISTRIBUTIONS FOR BASE-ISOLATED STRUCTURES

C. S. Tsai[1], Bo-Jen Chen[2], Tsu-Cheng Chiang[3], Wen-Shen Pong[4]

SUMMARY

The use of the base isolator to lengthen the natural period of a structure for reducing the transmission of energy from the ground into the structure has been recognized as an effective means by the engineering professions in earthquake prone regions. The seismic design of seismically isolated structures is mainly governed by the Uniform Building Code (UBC-97). The UBC code supplies a simple, statically equivalent design method where by displacements for an isolated structure are concentrated at the isolation level. Therefore, the superstructure nearly moves as a rigid body, and the design forces of elements above isolators are based on the behavior of isolators at the design displacement. However, in the UBC code, the distribution of inertial (or lateral) forces over the height of the superstructure above isolation has been found to be over-conservative for most isolated structures. In this paper, four simple and reasonable design formulae, based on the first mode of the base-isolated structure, for the lateral force distribution on the isolated structure have been validated by base-isolated steel structures tested on the shaking table. Moreover, to obtain more accurate results for irregular structures in which higher mode contributions are more likely expected during earthquakes, another four inertial force distribution formulae are also proposed to include the higher effect in this paper. Besides the experimental verification through shaking table tests, the recorded floor accelerations of the USC University Hospital during the Northridge earthquake were also adopted to investigate the suitability of the proposed design formulae considering the higher mode effect.

INTRODUCTION

[1] Professor, Department of Civil Engineering, Feng Chia University, Taichung, Taiwan, R.O.C.. Email:cstsai@fcu.edu.tw
[2] Ph. D., Assistant Research Fellow, Earthquake Proof System, Inc., Taichung, Taiwan, R.O.C.. E-mail:bjc@url.com.tw
[3] Ph. D. Candidate, Graduate Institute of Civil & Hydraulic Engineering, Feng Chia University, Taichung, Taiwan, R. O. C.. E-mail:rickchiang2001@yahoo.com.tw
[4] Assistant Professor, School of Engineering, San Francisco State University, U.S.A.. E-mail:wspong@sfsu.edu

The seismic upgrade design of seismically isolated structures is mainly governed by the Uniform Building Code (recently edition UBC-97) published by the International Conference of Building Officials (ICBO) [1-3]. The UBC code emphasizes that the displacements for a base-isolated structure are concentrated at the base isolation level, and that the superstructure almost moves as a rigid body and is designed for forces calculated using the effective stiffness of the isolation system at the design displacement. An equivalent static analysis procedure may be used for designing the bearings and the superstructure. Nevertheless, the distribution of lateral design forces over the height of the superstructure proposed in the UBC-97 is on the basis of an inverted triangular force distribution that is generally used for fixed-base structures. This distribution has been found to be the bound responses of most isolated structures conservatively, even when higher modes are excited by hysteretic behavior or large values of effective damping of the isolation system [3].

In recent years, this distribution of inertial (or lateral) forces over the height of the superstructure above isolation has been found to be the bound responses of most isolated structures conservatively, even when higher modes are generated by nonlinearities, large values of effective damping or the effects of friction in the isolation system. Tsai et al. [4-5], analytically based on the first mode of the base-isolated structure without complex calculation, have proposed two simple and reasonable design formulae for the lateral force distribution on an isolated structure. These two proposed design formulae assumes that the vertical distribution of inertia forces on an isolated structure should be a fashion of the first mode of the base-isolated structure rather than an inverted triangular force distribution suggested by the UBC code. Furthermore, in the UBC code, the weight of the base floor is ignored, which will overestimate the inertial force and maximum absolute acceleration on each floor. The proposed design formulae by Tsai et al. [4-5] also reasonably incorporate the influence of the inertial force on the base floor to calculate accurately the vertical distribution of inertial forces on a base-isolated structure.

In this paper, to obtain more accurate results for irregular structures in which higher mode responses are expected during earthquakes, there are another four inertial force distribution formulae proposed by considering higher modes of the base-isolated structures and the superstructures based on the theory of structural dynamics [6-10]. The effects of the first two modes of the base-isolated structure and the superstructure are included to improve accuracy of the lateral force distribution without surrendering simplicity. To compare the lateral force distributions computed from the proposed design formulae and UBC code provision, the experimental verification of a multiple-bay base-isolated steel structure in the shaking table tests at the National Center for Research on Earthquake Engineering in Taiwan has been carried out [11]. Besides the experimental verification through shaking table tests, the recorded floor accelerations of the USC University Hospital during the Northridge earthquake were also adopted to investigate the suitability of the proposed design formulae considering higher mode effects in this paper [12-13].

LINEAR THEORY OF BASE-ISOLATED STRUCTURES

In order to gain insight into the behavior of base-isolated structures, the linear theory of base isolation has already been developed by J. M. Kelly using a simple 2-DOF model with linear spring and linear viscous damping [6-7]. As shown in Fig. 1, one is the degree of freedom of the superstructure, and the other is the degree of freedom of the base isolator.

This 2-DOF system can be solved through modal decomposition to provide insight into the responses of base-isolated structures. The equation of motions is written in a matrix notation

$$\mathbf{M}\ddot{\mathbf{V}} + \mathbf{C}\dot{\mathbf{V}} + \mathbf{K}\mathbf{V} = -\mathbf{M}\mathbf{r}\ddot{u}_g \tag{1}$$

where

$$\mathbf{M}=\begin{bmatrix} M & m \\ m & m \end{bmatrix} \text{ A } \mathbf{C}=\begin{bmatrix} c_b & 0 \\ 0 & c_s \end{bmatrix} \text{ A } \mathbf{K}=\begin{bmatrix} k_b & 0 \\ 0 & k_s \end{bmatrix} \tag{2}$$

and

$$\mathbf{V}=\begin{bmatrix} v_b \\ v_s \end{bmatrix} \quad \text{A} \quad \mathbf{r}=\begin{bmatrix} 1 \\ 0 \end{bmatrix} \tag{3}$$

also

$$M = m + m_b \text{ A } v_b = u_b - u_g \text{ A } v_s = u_s - u_b \tag{4}$$

where m and m_b represent the mass of the superstructure (i.e., without base slab) and the mass of the base floor, respectively; c_b and k_b are the linear viscous damping coefficient and effective stiffness of the base isolator, respectively; c_s and k_s depict the damping coefficient and stiffness of the superstructure, respectively; u_s, u_b and u_g denote the absolute displacements of the superstructure, base isolator and the ground, respectively; M indicates the total mass of the superstructure plus that of the base floor; v_s represents the interstory drift of superstructure; v_b illustrates the isolation system displacement relative to the ground.

If the superstructure moves as a rigid body, the natural frequency of the isolated structure ω_b can be given by:

$$\omega_b = \sqrt{\frac{k_b}{M}} \tag{5}$$

The natural frequency of the fixed-base structure (i.e., without any isolation system) ω_s is

$$\omega_s = \sqrt{\frac{k_s}{m}} \tag{6}$$

Two important parameters are defined as

$$\varepsilon = \frac{\omega_b^2}{\omega_s^2} \quad , \quad \gamma = \frac{m}{M} \tag{7}$$

Moreover, the damping factors β_b and β_s given by

$$\beta_b = \frac{c_b}{2M\omega_b} \quad , \quad \beta_s = \frac{c_s}{2m\omega_s} \tag{8}$$

With the aid of Eqs. (1) and (2), the analytical solution of natural frequencies of the base-isolated structure can be given by [6-7]:

$$\omega_1^2 = \omega_b^2\left(1-\gamma\varepsilon\right) \quad , \quad \omega_2^2 = \frac{\omega_s^2}{1-\gamma}\left(1+\gamma\varepsilon\right) \tag{9}$$

and mode shapes are

$$\boldsymbol{\varphi}^1 = \begin{Bmatrix} 1 \\ \\ \dfrac{\varepsilon}{1-\gamma\varepsilon} \end{Bmatrix} \quad , \quad \boldsymbol{\varphi}^2 = \begin{Bmatrix} 1 \\ \\ -\dfrac{1+\gamma\varepsilon}{\gamma(1+\varepsilon)} \end{Bmatrix} \tag{10}$$

If $\gamma\varepsilon$ <<1, Eq. (10) can be rewritten as [6-7]:

$$\boldsymbol{\varphi}^1 = \begin{Bmatrix} 1 \\ \varepsilon \end{Bmatrix} \quad , \quad \boldsymbol{\varphi}^2 = \begin{Bmatrix} 1 \\ \\ -\dfrac{[1-(1-\gamma)\varepsilon]}{\gamma} \end{Bmatrix} \tag{11}$$

As shown in Fig. 2, the superstructure nearly moves as a rigid body in the first mode shape $\boldsymbol{\varphi}^1$; whereas in the second mode shape $\boldsymbol{\varphi}^2$, the displacements of the superstructure and the base isolator are opposite in direction. When the two modes, $\boldsymbol{\varphi}^1$ and $\boldsymbol{\varphi}^2$, are obtained, relative displacements, v_b and v_s, can be written as

$$v_b = q_1\phi_b^1 + q_2\phi_b^2 \quad , \quad v_s = q_1\phi_s^1 + q_2\phi_s^2 \tag{12}$$

where q_1, q_2 are time-dependent modal coefficients.

In most structural applications it is assumed that the damping is small enough and that effect of the off-diagonal components is negligible. The matrix equation (1) reduces to [6-7]

$$\ddot{q}_1 + 2\omega_1\beta_1\dot{q}_1 + \omega_1^2 q_1 = -L_1\ddot{u}_g \tag{13}$$

$$\ddot{q}_2 + 2\omega_2\beta_2\dot{q}_2 + \omega_2^2 q_2 = -L_2\ddot{u}_g \tag{14}$$

where

$$\beta_1 = \beta_b\left(1 - \frac{3}{2}\gamma\varepsilon\right) \ , \ \beta_2 = \left[\frac{\beta_s + \gamma\beta_b\varepsilon^{1/2}}{(1-\gamma)^{1/2}}\right]\left(1 - \frac{1}{2}\gamma\varepsilon\right) \tag{15}$$

and the participation factors, L_1 and L_2, for the first two modes in these equations are given by [6-7]

$$L_1 = 1 - \gamma\varepsilon \quad , \quad L_2 = \gamma\varepsilon \tag{16}$$

Then, the maximum values of q_1 and q_2 can be given by

$$|q_1|_{\max} = L_1 \, S_D(\omega_1 \, , \beta_1) \ , \ |q_2|_{\max} = L_2 \, S_D(\omega_2 \, , \beta_2) \tag{17}$$

where $S_D(\omega \, , \beta)$ is the displacement response spectrum for the ground motion, $\ddot{u}_g$, at frequency ω and damping ratio β.

If one normalizes the mode shapes of interstory drifts of the superstructure equal to 1. As shown in Fig. 3, with the aids of Eq. (10), then the mode shape of the 2-DOF model can be given by

$$\boldsymbol{\varphi}^1 = \begin{Bmatrix} \dfrac{1-\gamma\varepsilon}{\varepsilon} \\ \\ \\ 1 \end{Bmatrix} \quad , \quad \boldsymbol{\varphi}^2 = \begin{Bmatrix} -\dfrac{\gamma(1+\varepsilon)}{1+\gamma\varepsilon} \\ \\ \\ 1 \end{Bmatrix} \tag{18}$$

The vector of equivalent story shear forces can be written, based on the theory of structural dynamics, as [8]

$$\mathbf{F} = \begin{Bmatrix} f_1 \\ f_2 \end{Bmatrix} = \sum_{n=1}^{2} \omega_n^2 \mathbf{M}\boldsymbol{\varphi}_n |q_n|_{\max}$$

$$= \omega_1^2 \begin{bmatrix} M & m \\ m & m \end{bmatrix} \begin{Bmatrix} \dfrac{1-\gamma\varepsilon}{\varepsilon} \\ \\ 1 \end{Bmatrix} |q_1|_{\max} + \omega_2^2 \begin{bmatrix} M & m \\ m & m \end{bmatrix} \begin{Bmatrix} -\dfrac{\gamma(1+\varepsilon)}{1+\gamma\varepsilon} \\ \\ 1 \end{Bmatrix} |q_2|_{\max}$$

$$= \begin{bmatrix} m_b\left(\omega_1^2 C|q_1|_{\max} + \omega_2^2 D|q_2|_{\max}\right) + m\left(\omega_1^2|q_1|_{\max}(C+1) + \omega_2^2|q_2|_{\max}(D+1)\right) \\ \\ m\left(\omega_1^2|q_1|_{\max}(C+1) + \omega_2^2|q_2|_{\max}(D+1)\right) \end{bmatrix} \tag{19}$$

where

$$C = \frac{1-\gamma\varepsilon}{\varepsilon} = \frac{1}{\varepsilon} - \gamma \approx \frac{1}{\varepsilon} \left(\text{if } \gamma << \frac{1}{\varepsilon}\right) \tag{20}$$

$$D = -\frac{\gamma(1+\varepsilon)}{1+\gamma\varepsilon} \approx -\gamma[1+(1-\gamma)\varepsilon] \approx -\frac{\gamma}{[1-(1-\gamma)\varepsilon]} \left(\text{if } \varepsilon^2 << 1\right) \tag{21}$$

where f_1 and f_2 represent the base shear and story shear forces, respectively.

RATIONAL DESIGN FORMULAE FOR VERTICAL DISTRIBUTION OF LATERAL FORCES

In the UBC code, the lateral forces are assumed to be distributed over the height of the superstructure above the isolation interface in accordance with the formula [1-3]:

$$F_x = V_s \frac{w_x h_x}{\sum_{i=1}^{N} w_i h_i} \tag{22}$$

F_x depicts the inertia force at level x above the isolation level; w_x and w_i represent the weight at level x and level i, respectively; h_x, h_i are the heights of the xth and ith story above the isolation, respectively; V_s is the lateral seismic shear force; N is the total number of stories of the superstructure. The superstructure above the isolation system is designed and constructed to withstand a minimum shear force, V_s, using the formula

$$V_s = \frac{V_b}{R_I} \tag{23}$$

where

$$V_b = K_{D,\max} D_D \tag{24}$$

V_b represents the design force for the superstructure and the elements below the isolation interface; D_D depicts the design displacement of base isolation; $K_{D,\max}$ is the maximum effective stiffness of the base isolator at the design displacement; R_I portrays the design force reduction factor (ductility factor), which is intended to account for the inelastic response in the superstructure.

It is evident that Eq. (22) leads to a triangular vertical distribution of the inertia force over the height of the superstructure. Furthermore, the inertia force on each floor above the base floor computed from Eq. (22) seems to be overestimated because the weight of the base floor is neglected. In view of this, Tsai et al. [4-5] have proposed two rational and simple design formulae for the vertical distributions of the lateral

forces over the height of the superstructure while only considering the influence of the first mode of the base-isolated structure. The inertia force at each floor is given as (as shown in Fig. 2(a)) [4-5]

$$F_x = V_s \frac{w_x\left(1+\varepsilon\left(\frac{h_x}{H}\right)\right)}{\sum_{i=0}^{N} w_i\left(1+\varepsilon\left(\frac{h_i}{H}\right)\right)} \tag{25}$$

and

$$F_x = V_s \frac{w_x\left[1+\varepsilon\left(\phi_s^1\right)_x^*\right]}{\sum_{i=0}^{N} w_i\left[1+\varepsilon\left(\phi_s^1\right)_i^*\right]} \tag{26}$$

where $\varepsilon = \omega_b^2/\omega_s^2$ (see Eq. 7) is the ratio of natural frequencies, and also represents the ratio of the displacement at the top of superstructure relative to the base floor to that of the base floor (see Fig. 2(a)); H represents the total height of the base-isolated structure above isolation level; $\left(\varphi_s^1\right)^*$ represents the first mode shape of the fixed-base structure (i.e., without any isolator); $\left(\phi_s^1\right)_x^*$ and $\left(\phi_s^1\right)_i^*$ describe the values of the first mode shape at level x and level i, respectively, when the superstructure is rigidly fixed. It should noted that the value of the first mode shape at the top of the superstructure, $\left(\phi_s^1\right)_N^*$, should be normalized and equal to 1.

Moreover, if higher order terms of ε and $\gamma\varepsilon$ value are considered, Eqs. (25) and (26) can be rewritten as:

$$F_x = V_s \frac{w_x\left(1+\frac{\varepsilon}{1-\gamma\varepsilon}\left(\frac{h_x}{H}\right)\right)}{\sum_{i=0}^{N} w_i\left(1+\frac{\varepsilon}{1-\gamma\varepsilon}\left(\frac{h_i}{H}\right)\right)} \tag{27}$$

and

$$F_x = V_s \frac{w_x\left[1+\frac{\varepsilon}{1-\gamma\varepsilon}\left(\phi_s^1\right)_x^*\right]}{\sum_{i=0}^{N} w_i\left[1+\frac{\varepsilon}{1-\gamma\varepsilon}\left(\phi_s^1\right)_i^*\right]} \tag{28}$$

HIGHER MODE EFFECTS ON VERTICAL DISTRIBUTIONS OF LATERAL FORCES

The aforementioned four design formulae can obtain satisfactory predictions of the vertical distribution of inertia forces under cases mostly restricted to the superstructures that are almost rigid body motions and that the frequencies of the first and second modes on isolated structures are well-separated. Up to now, no any researcher accounts for the contributions of higher modes to the lateral force distributions of base-isolated structures if the superstructure is irregular or unsymmetrical and the structural systems are full of varieties. To overcome these liminations, suitable vertical distribution formulae for inertia forces by considering the second mode contribution of a base-isolated structure are proposed in this paper. With the aid of Eq. (19), two design formulae are given as:

$$F_x = V_s \frac{w_x \left[\omega_1^2 \left(\frac{1-\gamma\varepsilon}{\varepsilon} + \frac{h_x}{H} \right) + \omega_2^2 \frac{|q_2|_{\max}}{|q_1|_{\max}} \left(-\frac{\gamma(1+\varepsilon)}{1+\gamma\varepsilon} + \frac{h_x}{H} \right) \right]}{\sum_{i=0}^{N} w_i \left[\omega_1^2 \left(\frac{1-\gamma\varepsilon}{\varepsilon} + \frac{h_i}{H} \right) + \omega_2^2 \frac{|q_2|_{\max}}{|q_1|_{\max}} \left(-\frac{\gamma(1+\varepsilon)}{1+\gamma\varepsilon} + \frac{h_i}{H} \right) \right]} \tag{29}$$

and

$$F_x = V_s \frac{w_x \left[\omega_1^2 \left(\frac{1-\gamma\varepsilon}{\varepsilon} + \left(\phi_s^1\right)_x^* \right) + \omega_2^2 \frac{|q_2|_{\max}}{|q_1|_{\max}} \left(-\frac{\gamma(1+\varepsilon)}{1+\gamma\varepsilon} + \left(\phi_s^1\right)_x^* \right) \right]}{\sum_{i=0}^{N} w_i \left[\omega_1^2 \left(\frac{1-\gamma\varepsilon}{\varepsilon} + \left(\phi_s^1\right)_i^* \right) + \omega_2^2 \frac{|q_2|_{\max}}{|q_1|_{\max}} \left(-\frac{\gamma(1+\varepsilon)}{1+\gamma\varepsilon} + \left(\phi_s^1\right)_i^* \right) \right]} \tag{30}$$

where the maximum values of q_1 and q_2 can be obtained by numerical analyses [8]. In Eqs. (29) and (30), one chooses the same sign of q_1 and q_2 to ensure the flexibility of the superstructure, and it is also conformed to actual vertical distributions of inertia forces on isolated structures.

Moreover, in Eqs. (28) and (30), one can presume that the deflected shape of the superstructure relative to the base floor is the first mode shape $\left(\varphi_s^1\right)^*$ of the fixed-base structure (i.e., without any isolator). However, such satisfactory predictions are restricted to more like regular structures. It is very an important issue for an irregular structure to reasonably redistribute inertia forces on the superstructure by considering the contributions of higher modes on the superstructure [9]. To overcome these limitations, several researchers have proposed adaptive force distributions to provide better estimates of the fixed-base structure [9-10]. Chopra and Goel [9] have developed an improved modal pushover analysis (MPA) procedure. Jan et al. [10] have proposed an alternative method to simply estimate the lateral force distributions of high-rise buildings by combining contributions from the first and second modes. Based on proposed design formulae for the fixed-base structures by Chopra [8-9] and Jan et al. [10], one can combine the first- and second-mode contributions to obtain a distribution vector of the lateral force of the superstructure, and the distribution vector component is given as [8-10]:

$$\alpha_x = \frac{\omega_{s1}^2 w_x \left(\phi_s^1\right)_x^* + \omega_{s2}^2 \frac{\left|q_2^*\right|_{\max}}{\left|q_1^*\right|_{\max}} w_x \left(\phi_s^2\right)_x^*}{\omega_{s1}^2 w_N \left(\phi_s^1\right)_N^* + \omega_{s2}^2 \frac{\left|q_2^*\right|_{\max}}{\left|q_1^*\right|_{\max}} w_N \left(\phi_s^2\right)_N^*} \text{¡A}\left(x = 1 \text{ to } N\right) \tag{31}$$

where ω_{s1} and ω_{s2} depict the first- and second-mode natural frequencies of the fixed-base structure, respectively; w_x and w_N describe the weight at level x and level *N*, respectively; $\left(\phi_s^1\right)_x^*$ and $\left(\phi_s^2\right)_x^*$ represent the first- and second-mode shapes of the fixed-base structure at level x, respectively; $\left(\phi_s^1\right)_N^*$ and $\left(\phi_s^2\right)_N^*$ are the first- and second-mode shapes of the fixed-base structure at level *N* and are normalized to 1. It should noted that the value of the vector component at the roof level, α_N, should be equal to 1; and

$$\frac{\left|q_2^*\right|_{\max}}{\left|q_1^*\right|_{\max}} = \frac{\left|\Gamma_2 D_2\left(\omega_{s2}, \xi_2\right)\right|}{\left|\Gamma_1 D_1\left(\omega_{s1}, \xi_1\right)\right|} \tag{32}$$

where the nth-mode participation factor, Γ_n, is given by [8-10]

$$\Gamma_n = \frac{\left(\boldsymbol{\varphi}_s^n\right)^{*T} \mathbf{m}\boldsymbol{\nu}}{\left(\boldsymbol{\varphi}_s^n\right)^{*T} \mathbf{m} \left(\boldsymbol{\varphi}_s^n\right)^{*}} \tag{33}$$

where $\left(\boldsymbol{\varphi}_s^n\right)^{*}$ indicates the nth-mode shape of the fixed-base structure; $\mathbf{m}$ represents the mass matrix of the fixed-base structure; D_n represents the nth-mode spectral displacement; ξ_n denotes the nth-mode damping ratio of the fixed-base structure; $\boldsymbol{\nu}$ depicts the influence vector.

If one only considers the influence of the first mode of the base-isolated structure and simultaneously considers the first- and second-mode contributions of the superstructure, the design formula is given as:

$$F_x = V_s \frac{w_x \left[\dfrac{1-\gamma\varepsilon}{\varepsilon} + \alpha_x \right]}{\sum_{i=0}^{N} w_i \left[\dfrac{1-\gamma\varepsilon}{\varepsilon} + \alpha_i \right]} \tag{34}$$

Besides, to obtain more accurate results, one can take into account the influence of the second mode of the base-isolated structure and the higher mode contributions of the superstructure, and the design formula can be expressed as:

$$F_x = V_s \frac{w_x \left[\omega_1^2 \left(\dfrac{1-\gamma\varepsilon}{\varepsilon} + \alpha_x \right) + \omega_2^2 \dfrac{|q_2|_{\max}}{|q_1|_{\max}} \left(-\dfrac{\gamma(1+\varepsilon)}{1+\gamma\varepsilon} + \alpha_x \right) \right]}{\sum_{i=0}^{N} w_i \left[\omega_1^2 \left(\dfrac{1-\gamma\varepsilon}{\varepsilon} + \alpha_i \right) + \omega_2^2 \dfrac{|q_2|_{\max}}{|q_1|_{\max}} \left(-\dfrac{\gamma(1+\varepsilon)}{1+\gamma\varepsilon} + \alpha_i \right) \right]} \tag{35}$$

EXPERIMENTAL VERIFICATION FOR A MULTIPLE-BAY BASE-ISOLATED STRUCTURE

In order to verify the accuracy and suitability of proposed design formulae considering higher mode contributions of the isolated structure, a series of shaking table tests of a multiple-bay isolated structure were carried out, and given as an example to investigate the distinction among these proposed design formulae, the UBC code provision, and experimental results. As shown in Figs. 4 and 5, a 40% scale three-story base-isolated steel structure is constructed as a moment-resisting frame. The structure used for mounting base isolators is rectangular in shape, rising 4.25m vertically and occupying a plane of 4.5m × 4m horizontally. The weight from the base floor to the roof were approximately estimated equal to 108, 93, 93, and 85kN, respectively.

The isolation system was composed of five laminated rubber bearings (RB) and four stirrup rubber bearings (SRB) [11], as shown in Fig. 5. Figure 6 shows that the type of laminated rubber bearings tested is 146mm in diameter and 84mm in height. They consist of 10 rubber layers of 5mm thickness each, 9 steel plates of 1mm thickness each and 3mm rubber cover, and each end plate is 12.5mm thick with bolted connections. Figure 7 shows that the type of stirrup rubber bearing (noted as SRB) tested is also 146mm in diameter and 84mm in height. Each bearing consists of a lump of rubber materials of 54mm in thickness, 4 external steel rings of 6mm, 3mm rubber cover, and a plate of 15mm thickness at each end with bolted connections. The SRB bearing research conducted by Tsai in Taiwan, experimental examinations via the component and shaking table tests, indicate that the SRB bearing possesses higher damping ratios at higher strains, and lower horizontal effective stiffness than other kinds of rubber bearings even when the vertical axial load is slight.

The base-isolated structure was subjected to the 1940 El Centro earthquake in U. S. A. and the 1995 Kobe earthquake in Japan. The first two natural frequencies are 2.91Hz and 11.91Hz in the longitudinal direction of the structure without isolators. The mass ratio γ $(=m/M)$ is equal to 0.714. In this study, the main goal of experiments is to probe into the vertical distribution of lateral forces and verify the new proposed design formulae in comparison with the UBC code provision. Therefore, the design force reduction factor R_I is not included (i.e., $R_I = 1$) in this study. The magnitudes of the ε $(=\omega_b^2/\omega_s^2)$ value through the shaking table test are 0.1125 and 0.1381 during the El Centro and Kobe earthquakes, respectively. It shows the effectiveness of the rubber bearings mounted on this three-floor steel frame.

Tables 1 and 2 display the comparisons of results computed from the proposed design formulae, the UBC code provision, and the experimental studies in the longitudinal direction of the base-isolated frame during the El Centro and Kobe earthquakes. It is illustrated that the proposed design formulae can well predict the vertical distributions of the peak accelerations on the isolated structure during earthquakes. In the UBC code, the weight of the base floor is ignored, which will overestimate the maximum absolute acceleration on higher floors. Figures 8 and 9 depict the normalized peak accelerations on each floor calculated by Eqs. (25) and (35), the formula provided by the UBC code, and experimental results through shaking table tests. From these figures, it proves that results obtained from proposed design formulae are in good agreement with the experimental results. Moreover, it will be more accurate by considering higher mode effects of the base-isolated structure and the superstructure.

VERIFICATION OF PROPOSED FORMULAE THROUGH RECORDED DATA

In addition to the experimental verification, recorded floor accelerations for the University Hospital of the University of Southern California during the 1994 Northridge earthquake, as shown in Figs. 10 and 11 [12-13], are adopted to investigate distinctions among the proposed design formulae, UBC code provision, and recorded data. The peak free-field and peak foundation accelerations in the north-south direction were 0.49g and 0.37g, respectively. The maximum floor accelerations were recorded at the base and the roof of the hospital to be 0.13g and 0.21g, respectively. The peak floor accelerations were also recorded at the 4th floor and 6th floor to be 0.10g and 0.11g, respectively. In this study, linear interpolation is utilized to obtain other floor accelerations without instrumentation. The mass from the base floor to the roof were equal to 33.275, 14.874, 13.709, 12.354, 12.233, 12.146, 9.769, 8.897, 10.942 $kip \times \sec^2/in$, respectively. The first two natural frequencies are approximately 1.93Hz and 4Hz in the north-south direction of the fixed-base USC University Hospital.

The mass ratio γ $(=m/M)$ is equal to 0.74, and the magnitude of the ε $(=\omega_b^2/\omega_s^2)$ value is equal to 0.15. Table 3 exhibits the comparisons of results calculated from the UBC code provision, the proposed design formulae, and the recorded acceleration data in the north-south direction of the USC University Hospital. It is illustrated that the vertical distributions of peak accelerations computed by proposed design formulae are in good agreement with the recorded floor accelerations. Figure 12 illustrates the normalized peak accelerations on each floor calculated by Eqs. (25) and (35), the formula provided by the UBC code, and the recorded acceleration data. It demonstrates that the proposed design formulae can well predict the vertical distributions of peak accelerations in actual earthquakes. When the higher mode effect is considered, better agreement with the recorded data is observed. Furthermore, it also demonstrates that the acceleration at each floor calculated by the UBC code provision has been found to be distinct considerably in contrast with the recorded acceleration data and too conservative.

CONCLUSIONS

The design of seismically isolated structures is mainly governed by the Uniform Building Code (UBC) published by the International Conference of Building Officials. Nevertheless, the vertical distributions of lateral forces over the height of the superstructure in the UBC code provision is on the basis of an inverted triangular force distribution. It has been found to be the bound responses of most isolated structures conservatively, even when higher mode contributions are generated. The design formulae proposed in this paper can reasonably incorporate the influence of the inertial force on the base floor to accurately calculate the lateral force distributions on isolated structures via the verification of the experimental and recorded data. Meanwhile, the proposed design formulae considering higher mode effects are in good agreement with the actual vertical distributions of lateral forces on irregular base-isolated structures.

ACKNOWLEDGEMENT

Special thanks is given to the National Science Council, Taiwan, R. O. C., for financial support for this research (NSC 90-2211-E-035-016). The assistance from the National Center for Research on Earthquake Engineering in Taiwan and KPFF Consulting Engineerings in U. S. A. are appreciated.

REFERENCES

[1] Uniform Building Code, International Conference of Building Officials, Whilter, California, 1997.
[2] NEHRP Guidelines for the Seismic Rehabilitation of Buildings, Federal Emergency Management Agency, FEMA-273, 1993.
[3] NEHRP Guidelines for the Seismic Rehabilitation of Buildings, Federal Emergency Management Agency, FEMA-274, 1994.
[4] C. S. Tsai, Bo-Jen Chen and Tsu-Cheng Chiang " Experimental and Computational Verification of Reasonable Design Formulae for Base-Isolated Structures." Earthquake Engineering and Structural Dynamics, Vol. 32, 1389-1406.
[5] C. S. Tsai, Bo-Jen Chen and Tsu-Cheng Chiang " Reasonable Lateral Force Distributions on Isolated Structures." The 2002 ASME Pressure Vessels and Piping Conference, Seismic Engineering 2002, Vancouver, British Columbia, Canada, Vol. 2, pp. 229-236, August 2002.
[6] James M Kelly " Earthquake-Resistant Design with Rubber." Second Edition, Springer-Verlag, London, 1997.
[7] Farzad Naeim and James M. Kelly " Design of Seismic Isolated Structures: From Theory to Practice." John Wiley & Sons, Inc., 1999.
[8] Anil. K. Chopra " Dynamics of Structures: Theory and Applications to Earthquake Engineering." Prentice-Hall, Inc., 1995.
[9] Anil. K. Chopra and Rakesh K. " A Modal Pushover Analysis Procedure for Estimating Seismic Demands for Buildings" Earthquake Engineering and Structural Dynamics, Vol. 31, pp. 561-582, 2001.
[10] T. S. Jan, M. W. Liu and Y. C. Kao " Pushover Analysis and Seismic of Structures to Near Fault Earthquake." A Research Report of National Council of Taiwan, Report No: NSC 90-2211-E-035-014, Sept. 2002.
[11] C. S. Tsai, Bo-Jen Chen, Tsu-Cheng Chiang and Guan-Hsing Lee " Experimental Study of a Multiple Bay Structure Isolated With Hybrid Bearings." The 2003 ASME Pressure Vessels and Piping Conference, Seismic Engineering 2003, Cleveland, Ohio, U.S.A., pp. 89-96, July 2003.
[12] Jefferson W. Asher, David R. Van Volkinburg, Ronald L. Mayes, Trevor Kelly, Bjorn I Sveinsson and Saif Hussain " Seismic Isolation Design of the USC University Hospital" Proceedings of Fourth U.S. National Conference on Earthquake Engineering, Palm Springs, California, U. S. A., Vol. 3, May, 1990.
[13] Petros Komodromos " Seismic Isolation for Earthquake-Resistant Structures." WIT Press, Southampton, Boston.

Tab. 1 Acceleration Comparisons of Results Obtained from Proposed Design Formulae, UBC Code Provision, and Experiment in Longitudinal Direction of Base-Isolated Structure during El Centro Earthquake

Excitation		BASE	1F	2F	ROOF
El Centro PGA=0.6010g	Equation (25)	0.3214	0.3349	0.3462	0.3575
	Equation (26)	0.3206	0.3351	0.3479	0.3566
	Equation (27)	0.3199	0.3346	0.3468	0.3591
	Equation (28)	0.3187	0.3360	0.3481	0.3577
	Equation (29)	0.3095	0.3323	0.3512	0.3701
	Equation (30)	0.3077	0.3344	0.3532	0.3680
	Equation (34)	0.3238	0.3276	0.3454	0.3634
	Equation (35)	0.3154	0.3213	0.3491	0.3771
	UBC Code	N/A	0.2873	0.5268	0.7662
	Experimental Results	0.3044	0.3085	0.3446	0.4102

Units: g

Tab. 2 Acceleration Comparisons of Results Obtained from Proposed Design Formulae, UBC Code Provision, and Experiment in Longitudinal Direction of Base-Isolated Structure during Kobe Earthquake

Excitation		BASE	1F	2F	ROOF
Kobe PGA=0.7008g	Equation (25)	0.2676	0.2799	0.2901	0.3003
	Equation (26)	0.2668	0.2800	0.2916	0.2995
	Equation (27)	0.2662	0.2796	0.2907	0.3019
	Equation (28)	0.2651	0.2808	0.2919	0.3006
	Equation (29)	0.2564	0.2774	0.2948	0.3123
	Equation (30)	0.2548	0.2793	0.2966	0.3103
	Equation (34)	0.2733	0.2678	0.2868	0.3100
	Equation (35)	0.2673	0.2586	0.2888	0.3256
	UBC Code	N/A	0.2403	0.4406	0.6409
	Experimental Results	0.2894	0.2523	0.2739	0.3205

Units: g

Tab. 3 Acceleration Comparisons of Results Obtained from Proposed Design Formulae, UBC Code Provision, and Recorded Acceleration Data in North-South Direction of USC University Hospital during Ground Motions

	Base	1F	2F	3F	4F	5F	6F	7F	8F
Eq. (25)	0.120	0.122	0.124	0.126	0.129	0.131	0.133	0.136	0.138
Eq. (26)	0.122	0.123	0.123	0.124	0.125	0.128	0.132	0.137	0.141
Eq. (27)	0.118	0.121	0.124	0.126	0.129	0.132	0.135	0.137	0.140
Eq. (28)	0.121	0.122	0.123	0.124	0.125	0.129	0.133	0.138	0.143
Eq. (29)	0.110	0.115	0.121	0.126	0.132	0.137	0.143	0.148	0.154
Eq. (30)	0.115	0.117	0.119	0.121	0.123	0.131	0.141	0.151	0.161
Eq. (34)	0.128	0.124	0.120	0.118	0.117	0.120	0.129	0.138	0.151
Eq. (35)	0.131	0.119	0.111	0.107	0.104	0.111	0.132	0.153	0.183
UBC Code	N/A	0.041	0.082	0.123	0.163	0.204	0.245	0.286	0.327
Recorded Data	0.130	0.122	0.115	0.109	0.104	0.105	0.106	0.149	0.205

Units: g

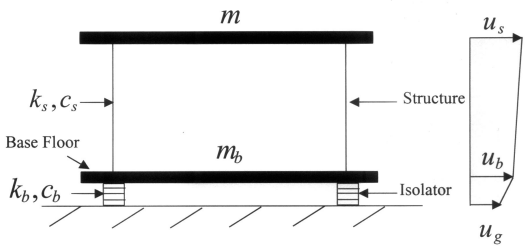

Fig. 1 Two-Degree-of-Freedom Base Isolation System

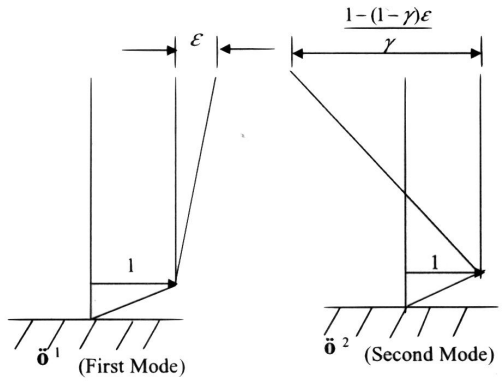

(a) (b)

Fig. 2 Mode Shapes of Two-Degree-of-Freedom Base Isolation System

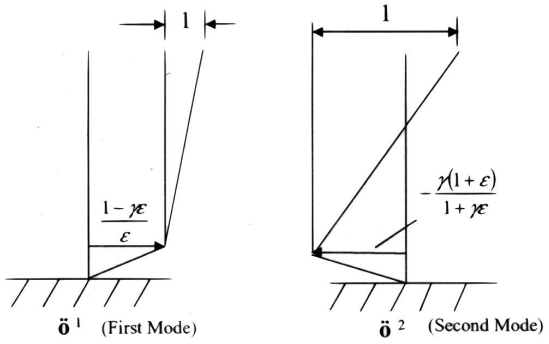

(a) (b)

Fig. 3 Mode Shapes of Two-Degree-of-Freedom Base Isolation System

Fig. 4 Tested Base-Isolated Structure

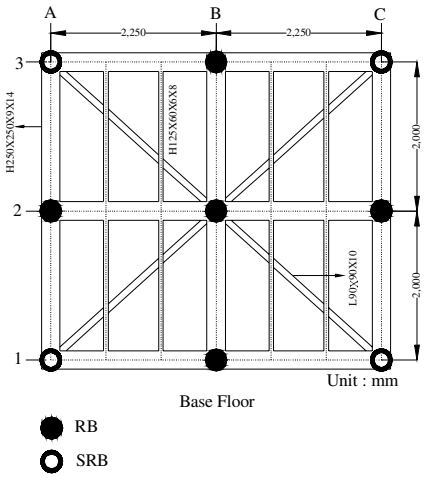

Fig. 5 Location of Rubber Bearings

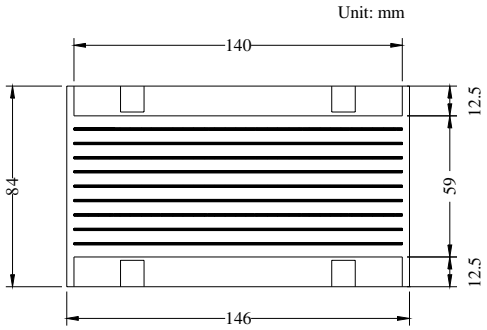

Fig. 6 Schematic of Laminated Rubber Bearing (RB)

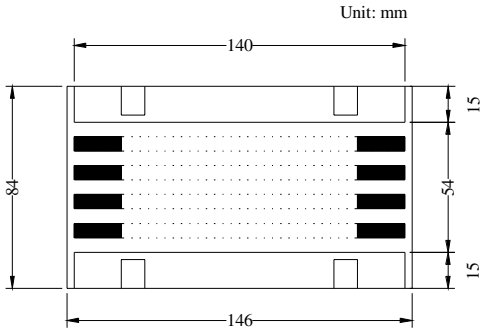

Fig. 7 Schematic of Stirrup Rubber Bearing (SRB)

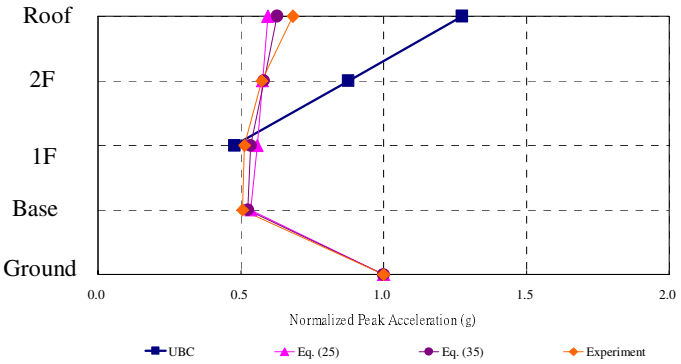

Fig. 8 Comparisons of Normalized Peak Story Accelerations of Multiple-Bay Isolated Steel Structure under El Centro Earthquake (PGA=0.6010g)

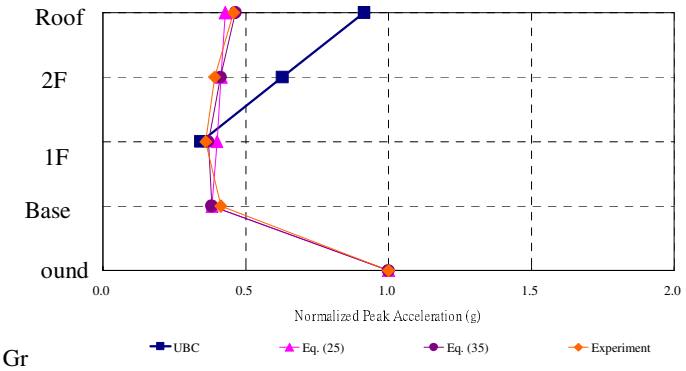

Fig. 9 Comparisons of Normalized Peak Story Accelerations of Multiple-Bay Isolated Steel Structure under Kobe Earthquake (PGA=0.7008g)

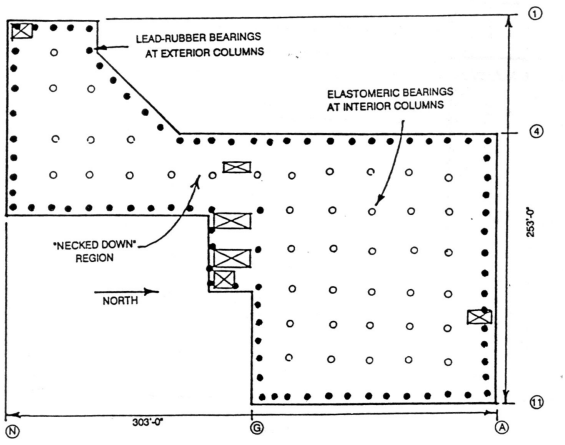

Fig. 10 USC University Hospital Floorplan

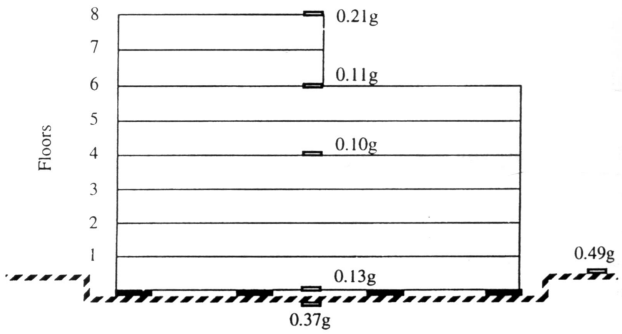

Fig. 11 Recorded Floor Accelerations of USC University Hospital

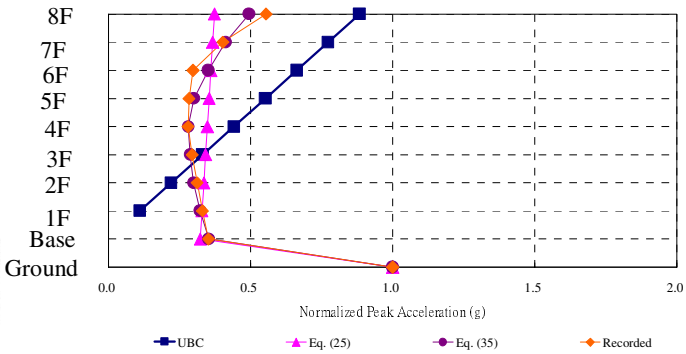

Fig. 12 Comparisons of Normalized Peak Story Accelerations of USC University Hospital under 1994 Northridge Earthquake